EFFICIENT PHYSICAL MODELLING OF DISTRICT HEATING NETWORKS

ABSTRACT
A mathematical physical model for dynamic simulation of flow and temperature in district heating networks (DHN) is proposed. The network structure is described by means of a graph-theoretical approach where the network elements are pipe sections, consumers and heat sources. The governing equations for hydraulic flows and heat distribution through pipe networks are presented. In addition, proper orthogonal decomposition is outlined and applied for obtaining a reduced model representation of the hydraulic equations. It is shown that the proposed methods are suitable for predicting flow and temperature values at each consumer with minimal average error and can therefore be used as a conceptual tool for operational optimization of district heating networks.

KEY WORDS
Dynamic Modelling, District heating systems, Thermal problems, Projection-based model reduction, Graph theory, Physically-based Modelling.

1 Introduction

The interest in DHN has grown substantially in recent years. This is mainly due to environmental issues, such as the necessity in reduction of carbon dioxide emissions. The purpose of DHN is to supply adequate heat to its consumers by utilizing production plants and a network of pipes for distribution. One advantage of such centralized heating production plants is that reducing emissions and limiting pollution is more effectively accomplished than in local installations at the consumers. However, major difficulties arise in operational planning due to large transport delays from the centralized heating plant to the consumer stations. To meet the heat demand of a consumer at a specific time t_k successfully, it is already necessary to "know" the demand at time $t_{k-\tau}$, where τ represents the transport delay, which is a function of the speed of the flow in the network. This motivates the use of statistical models to predict the heat demand. Long transportation times of the heat from the plant to the consumer also result in high heat losses in the network which from a cost point of view should be kept small. The literature is full of studies about sophisticated approaches, attempting to model or predict the dynamical behavior of district heating networks. However, the vast majority of these proposed methods are data driven [1, 2, 3] and can be settled into the category of Black Box Models, which, by definition, do not take the underlying physical structure into account. Also few attention is paid to variable transport delays in DHN. For instance, in [2] the network dynamics are part of the stochastic component. A static optimization of DHN is proposed in [6], where transport delays are considered but held constant during the simulation. In [4] a steady state and a dynamic model were set up, in which each consumer installation is described separately by a heat exchanger with primary and secondary network combined with a flow regulator controlling the indoor temperature. Model reduction issues for large-scale networks were discussed in [5]. The authors proposed an aggregation approach for constructing equivalent networks based on physical conservation laws.
This paper presents a fully dynamical physical model for simulating the hydraulic, thermal behavior of DHN. Furthermore, variable transport delays are considered and consumer installations are modelled as combined time-varying thermal and hydraulic resistances, where the resistive value depends on the actual heat load of the consumer. Model reduction is achieved efficiently by means of proper orthogonal decomposition. Finally, the full model and the reduced model are applied to the test case of the Tannheim district heating system.

2 Physical Model

2.1 General Model Structure

DHN are typically composed of many elements, building a supply chain from heat sources to heated buildings. The elementary components may be broken down to a heat production facility DHP, consumers acting as sinks, and pipes needed for heat transportation by water. The plant itself may be considered as the interaction of a pump to ensure certain pressures of the flow in the network, and a boiler for heating the flow to specific temperatures. Pressure drop (head losses) and thermal losses in the network are accounted for by corresponding pipe and heat resistor values. The heat energy balance in a DHN can be stated as the following

$$Q_s = Q_{loss} + \sum_{i=1}^{N} Q_{c_i} \tag{1}$$

with

$$\begin{aligned} Q_s &= c_p \dot{m}(T_s - T_r) \\ Q_{loss} &= hA(\tilde{T}_s - T_g) \\ Q_{c_i} &= c_p \dot{m}_{c_i}(T_{s_{ci}} - T_{r_{ci}}) \end{aligned} \tag{2}$$

At optimal conditions the energy Q_s produced at the supply point is equal to the sum of the individual heat loads of the consumers Q_{c_i} and thermal losses Q_{loss}. The latter can be interpreted as a function of the ground temperature T_g, some average network supply temperature $\tilde{T}_s$, pipe surface area A and heat transfer coefficient h. The heat load at the consumer is specified by the temperature difference between supply line and return line $T_{s_{ci}} - T_{r_{ci}}$ multiplied with the mass flow through the consumer installation $\dot{m}_{c_i}$ and the specific heat capacity of water c_p. Considering equations (2), one can easily derive that $dQ_c/dT_{s_c} > 0$ $(c_p \dot{m}_c > 0)$. Hence, heat energy at consumer installations can be increased by raising the temperature of the supply line. However, increased temperature in the supply line is proportional to higher thermal losses. On the other hand, cost of pumping can significantly be reduced by lowering the mass flow rates. Figure 1 illustrates the physical components of DHN but also provides some basic insight into the circular structure of district heating networks. Here the mass flow rate $\dot{m}$ may be calculated from the functional relationship between pressure at the plant DHP, the resistive values of the two supply pipes P_{1s}, P_{2s}, the two return pipes P_{1r}, P_{2r}, and the consumer being represented as variable resistor R_c. This relationship is comprehensively discussed in subsection 2.2 and in the simulation part, chapter 3. The motivation for the variable resistor R_c arises from the fact that flow regulators installed at the consumer stations are trying to keep the return temperature at constant value by controlling the opening degree of the valve. For the thermal part the supply temperature at the plant T_s and the heat losses at the pipes are important. This issue is further addressed in subsection 2.4.

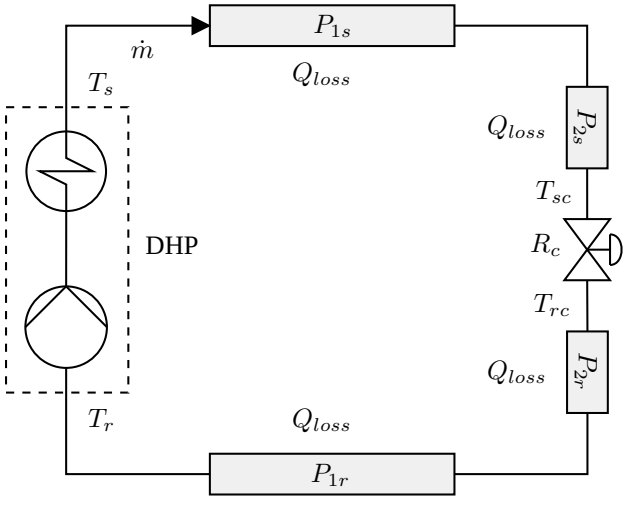

Figure 1: Sample network.

2.2 Hydraulic Part

Due to the assumption of incompressible media, the computation of flow distributions in DHN are mainly based on the so called *Kirchhoff* equations. The first Kirchhoff equation states that the algebraic sum of all the currents at any node is equal zero and the second law states that the sum of the pressure losses along a mesh is zero. First, consider the partial differential equation describing an one dimensional flow through a horizontal pipe which can be systematically derived from the Navier-Stokes equation.

$$\frac{l}{A}\frac{d\dot{m}}{dt} + \Delta p + R|\dot{m}|\dot{m} = 0. \tag{3}$$

Note that (3) has already been discretized spatially, with Δp denoting the difference in pressure head between the two pipe ends and $\dot{m}$ the mass flow rate. The variable R stands for the hydraulic resistance of the pipe element, which is postulated to be a function of the physical properties such as length, roughness and diameter [8].
A suitable method for describing the topology of DHN is to apply the basic concepts of graph theory. First of all, the layout of the so called incidence matrices is briefly reviewed. Assuming a tree network with n_n nodes (one plant, n_c consumers and interior nodes) and n_b branches. The incidence matrix $\mathbf{A}$ is a matrix of size $n_b \times n_n$ populated with entries a_{ij} where

$$a_{ij} = 1 \text{ if pipe } i \text{ starts at node } j;$$
$$a_{ij} = -1 \text{ if pipe } i \text{ ends at node } j;$$
$$a_{ij} = 0 \text{ otherwise.}$$

If consumer flows $Q \in \mathcal{R}^{n_c}$ are known or are obtained from expressions (2), the calculation of the flow distribution $\dot{m} \in \mathcal{R}^{n_b}$ in the network reduces to solving the system of linear equations (4), where $\mathbf{A_i}$ denotes the interior node incidence matrix (consumer plus interior nodes) with properly grouped consumer nodes.

$$\mathbf{A_i}'\dot{m} = \begin{pmatrix} Q \\ 0 \end{pmatrix} \tag{4}$$

However, in the case of unknown consumer flows a solution may be obtained by applying the *Principle of D'Alembert*. Formulation (3) can be restated in matrix form as differential algebraic expression (DAE)

$$\mathbf{K}\frac{d\dot{m}}{dt} + \mathbf{B}p + \mathbf{R}|\dot{m}|\dot{m} = 0 \tag{5}$$
$$s.t. \quad \mathbf{A_i}'\dot{m} = 0.$$

Here the incidence matrix should comprise both supply and return line, which means that instead of working with the tree network the entire distribution loop is considered. Multiplying (5) with $\delta\dot{m}' = (\mathbf{T}\delta q)'$, the so called virtual displacements, and substituting $\mathbf{T}q$ for $\dot{m}$ where $\mathbf{T} = \ker(\mathbf{A_i}')$ in both cases yields

$$\delta q'\mathbf{T}'\mathbf{K}\mathbf{T}\dot{q} + \delta q'\mathbf{T}'\mathbf{B}p + \delta q'\mathbf{T}'\mathbf{R}|\mathbf{T}q|\mathbf{T}q = 0$$
$$\delta q'(\tilde{\mathbf{K}}\dot{q} + \tilde{\mathbf{B}}p + \tilde{\mathbf{R}}|\mathbf{T}q|\mathbf{T}q) = 0. \tag{6}$$

Thus, the DAE (5) was successfully transformed into an ordinary differential equation (ODE) (6) which can be solved by various integration schemes. Specifically, in this work, the semi-implicit Rosenbock method [12] was found to be appropriate.

2.3 POD of Hydraulic Part

With growing networks and/or longer simulation horizons it becomes necessary to pay attention to techniques trying to decrease the computational burden by model reduction. This can be achieved by means of the so called proper orthogonal decomposition (POD) approach [9]. Here it is assumed that the pipe flow in the network may be determined by certain dominant characteristics. The main idea is to monitor time instances (snapshot ensemble) of the flows in the branches in DHN over a period and to seek for patterns, or, technically spoken, to seek for a set of orthogonal basis functions which describe most of the dynamical behavior. Assume the full model has been simulated over a time interval, N snapshots are collected and the snapshot matrix $\mathbf{X} \in \mathcal{R}^{N \times n_b}$ is populated, so that the i^{th} row corresponds to the i^{th} snapshot. Next, the eigenvalue decomposition of the $n_b \times n_b$ correlation matrix of $\mathbf{X}$ is computed. A POD basis of rank l is obtained by projecting the data vectors onto the first $l < n_b$ unit norm eigenvectors

$$u_j = \mathbf{X} v_j \quad \text{for } j = 1, \ldots, l \tag{7}$$

where v_j is the j^{th}eigenvector and u_j's are the orthogonal eigenfunctions (modes). Hence, q in (6) can be replaced by a reduced state vector $\zeta = \mathbf{V}' q$.

2.4 Thermal Part

In the dynamic simulation the thermal process is completely separated from the hydraulic part, due to different time dynamics and different response times, which also makes the problem from a numerical point of view difficult to solve. The flow is driven by pressure waves and reaches steady state typically in a matter of seconds, whereas temperature changes at the plant may need hours to reach consumer stations. The response time is solely determined by the speed of the flow. Hence, the hydraulic part is solved first and the resulting (steady state) flows specify the transport dynamics in the temperature equation, which may be formulated in the following way

$$C \frac{dT}{dt} = \dot{m} c_p (T^*_{in} - T) - H_r (T - T_g). \tag{8}$$

$T = T(t)$ and $T^*_{in} = T_{in}(t - \tau)$ denote the temperatures of the fluid at the outlet of the pipe at time t and the inlet of the pipe at $t - \tau$, respectively. The variable c_p denotes the specific heat capacity of the fluid and C measures the total heat capacity of the pipe. The last term in (8) accounts for the energy losses to the surroundings, where H_r stands for the heat/thermal resistance, which is, amongst others, a function of the pipe surface area and some heat loss coefficient. The time delay τ can be calculated from

$$\int_{t-\tau}^{t} \frac{4\dot{m}(\zeta)}{\pi D^2 \rho} d\zeta = L, \tag{9}$$

with L and D denoting the length and diameter of the pipe segment, respectively and ρ the density of water. Similarly to the hydraulic part, the spatial discretization is performed in such way that the grid points are the inflow and outflow nodes of the pipe sections. Thus, instead of computing the temperature characteristics along the pipe only the temperature profile at particular nodes is of interest. This means, for instance, that the temperature of the outflow node is obtained by addressing the time history of the inflow node, which in turn has to be approximated. This approach is also referred to as the node method [7, 11]). Here, at every time step, the time delays are calculated from the mass flow time histories and on the basis of this as well as heat losses and heat capacities of the pipes the temperature at each node in the network has to be updated. For determining the connection structure among the nodes the incidence matrix discussed in subsection 2.2 is utilized. Equation (8) can be solved by applying appropriate explicit or implicit integrations schemes. The so called *Courant number* [10] plays a crucial role in this context, and should therefore be investigated more closely in further stability analysis. In this work the differential equation (8) was solved with the implicit Backward Euler scheme.

3 Case-study Tannheim

3.1 DHN Structure and Assumptions

The methods are applied to the test case of the Tannheim district heating net (see fig. 11). Tannheim is located in Tyrol in Austria and is a typical tourist center with about 1100 inhabitants. The heat distribution loop is a 14km long pipeline system with one single heat production facility. Today, 84 building objects, mainly consisting of private houses, few hotels and some guest houses, are connected to this system. In fig. 2 the supply pipe dimension characteristics are depicted. One can easily observe that thin pipes in terms of diameter (DN25-DN40; DN...Diameter Nominal) are mainly used as a connector to the individual consumer stations and are therefore tending to be shorter than the main distribution network. A symmetric network structure between supply and return pipes is assumed, i.e. physical properties such as length or diameter are identical for supply and return line. The data for simulation consist of measurements of temperature at the district heating plant, as well as measurement of temperatures, mass flows and heat loads at the consumer stations. The time horizon of the data set is from 10.1. - 12.1.2009 with a resolution of 15 minutes. The pipe head losses were determined by the *Darcy-Weisbach* formula

$$R_{p_i} = f_r \frac{L_i}{D_i} \frac{1}{2\rho A_i^2}, \tag{10}$$

with appropriate chosen friction factor f_r [8, p.357] and the resistance values of the consumer installations are modelled as

$$R_{c_i} = k_i \frac{\sum_{i=1}^{N} Q_i^2}{Q_i^2}, \tag{11}$$

where the k_i's are tuning parameters. The idea of this approach is that the resistor values should somehow be inversely proportional to the (scaled) heat load. The quadratic nature originates from equation (3). For stability reasons the corresponding mass flow rate is $m_{c_i} = 0$, if R_{c_i} is bigger than some a-priori defined R_{max}. The heat

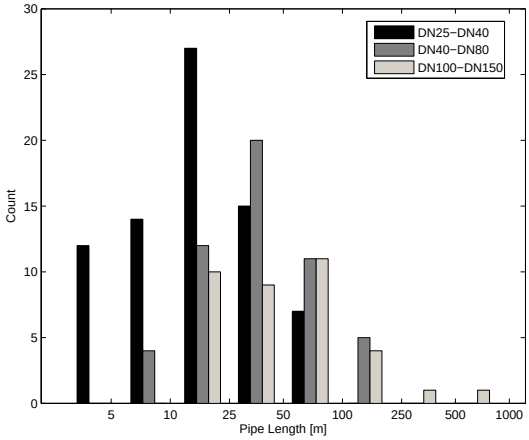

Figure 2: Supply pipes characteristics.

resistance for each individual pipe for the thermal simulation is chosen as the following

$$R_{Hr_i} = h\,\pi D_i L_i, \tag{12}$$

where h denotes the heat transfer coefficient. The assumption that thermal losses are a function of pipe surface area and time delays is clearly confirmed by observing figs. 3 and 4. Fig. 3 demonstrates that the farther the consumers are away from the plant in terms of pipe lengths the lesser are the mean supply temperatures and the latter shows that the mean temperature also depends on the average time delays in the network. Furthermore, it is important to men-

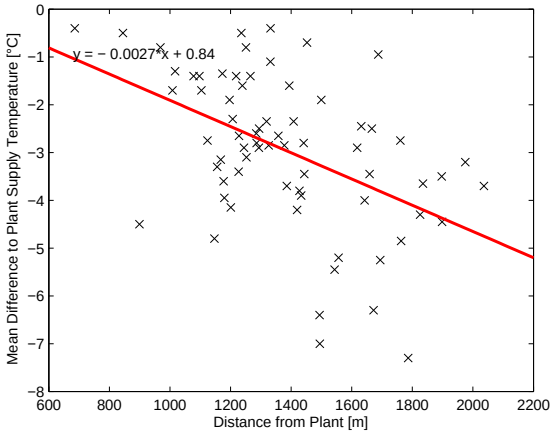

Figure 3: Temperature loss against distance.

tion that the pressure at the plant is assumed to be constant, due to the fact that unfortunately no data was available.

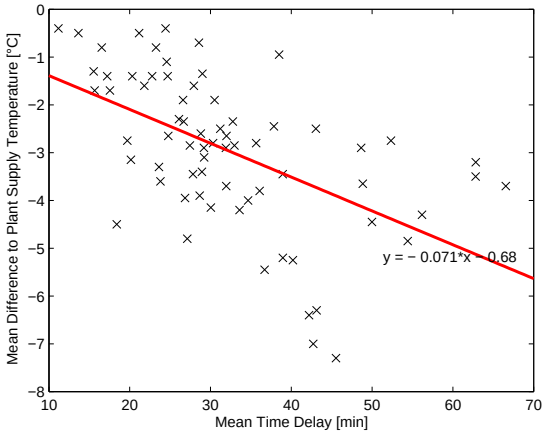

Figure 4: Temperature loss against transport time delay.

3.2 Simulation Results and Discussion

The first part of the dataset, comprising one day of data, acts as training set for finding optimal tuning and physical parameters, and the remaining measurements are used for testing. For visualization purposes only the simulation results of two consumer stations are considered, namely a hotel with an average heat load of about 500 kW being by far the largest consumer (consumer 1) and a private house with an average heat load of 46 kW being a medium-sized consumer (consumer 2). All modelling was performed with MATLAB version 7.10 and as a computing platform an Intel Core i5 Intel Processor 2.53GHz with 3GB system memory was available. The typical CPU simulation time for the hydraulic simulation is about 280s compared to 60s for the thermal simulation. Some basic statistics are summarized in table 1. The average error and standard devia-

Table 1: Statistical properties of simulated and reference mass flow rates [kg/s].

		Simulation	**Reference**
Con 1	*Mean*	5.487	5.561
	Std. Deviation	0.673	0.880
Con 2	*Mean*	0.308	0.319
	Std. Deviation	0.0623	0.0714

tion (in brackets) sums up to -0.0738 kg/s (0.682 kg/s) for consumer 1 and -0.0107 kg/s (0.0582 kg/s) for consumer 2, respectively. The standard deviation of the error is somewhat high, which may be caused by the unknown pressure variations at the plant. From figure 5 and 6 one can also observe that some peaks do not match. It can be argued that this may be due to not considering pressure fluctuations on the one hand and abrupt changes in the supply temperature on the other hand. The latter is indirectly included in the simulation process through the heat load (see equ. (2)). This issue could be resolved by filtering supply temperature effects from the heat load data or by incorporating

additional terms into the consumer resistor formula (11).

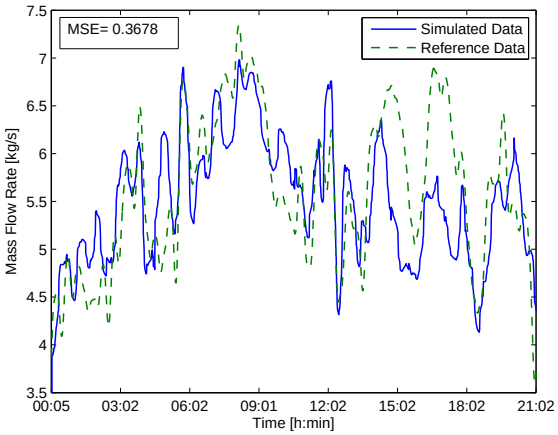

Figure 5: Simulated and reference mass flow rates for consumer 1.

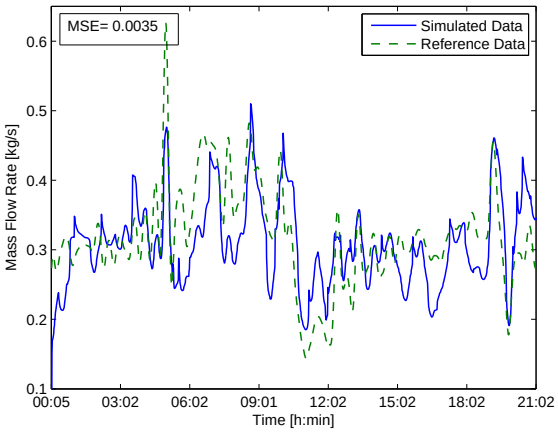

Figure 6: Simulated and reference mass flow rates for consumer 2.

As can be seen in fig. 7, only 6 modes out of 84 of the POD-model described in subsection 2.3 are needed to capture more than 90% of the total variation in the data. In fig. 7 the hydraulic simulation results for a POD basis of rank 6 are plotted. The extreme up- and downtrends are not well reproduced, but the trend following ability is acceptable.

Results for the thermal simulation part are summarized

Table 2: Statistical properties of simulated and reference supply temperature [$^{\circ}C$].

		Simulation	**Reference**
Con 1	*Mean*	86.02	85.89
	Std. Deviation	1.23	2.29
Con 2	*Mean*	83.053	83.046
	Std. Deviation	1.22	1.95

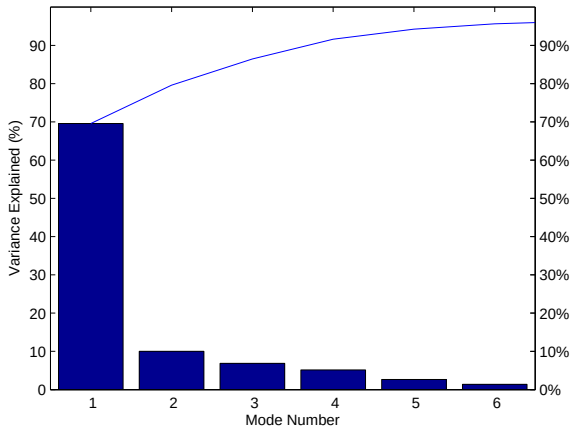

Figure 7: Scree plot of the percent variability explained by the corresponding modes.

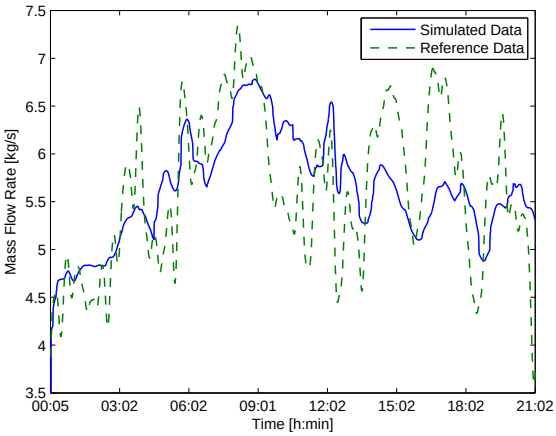

Figure 8: Simulation results with reduced model representation for consumer 1.

in table 2 and visualized in figs. 9 and 10. The average error was calculated to be -0.0733 °C with standard deviation 2.3 °C for consumer 1 and $0.0165^{\circ}C$ with standard deviation $2.23^{\circ}C$ for consumer 2, respectively. Despite the small average error, the relatively high standard deviation shows that the simulation is hardly able to follow the dynamics of the reference supply temperature. It seems, especially for consumer 2 being farther away from the plant than consumer 1, that there is no systematic relationship of the transient behavior in the supply temperature. One reason for this is that no detailed information about the value of the heat capacities of the individual pipe elements was available. The intention behind these capacities is to smooth out transient fluctuations in the supply temperature. Direct estimation of the parameters using for instance least squares methods would certainly lead to improvements. A detailed analysis in this direction will be attempted in future publications. Furthermore, as a measure for global efficiency of the DHN in Tannheim the total heat loss in the network

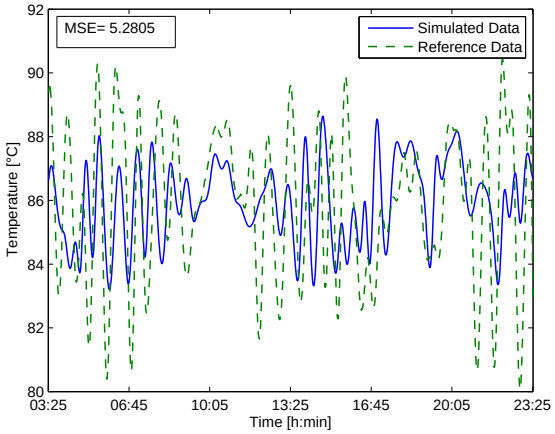

Figure 9: Simulated and reference supply temperature profile at consumer 1.

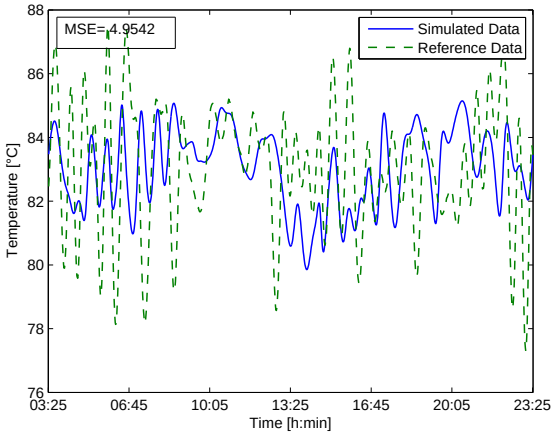

Figure 10: Simulated and reference supply temperature profile at consumer 2.

can be related to the total consumed heat by the following expression $(1-Q_{loss}/\sum Q_{c_i})\cdot 100$. For this specific simulated time horizon the global efficiency was calculated to be 86.1%, which means that about 14% of the heat produced at the plant during this period is lost to the surroundings.

4 Conclusion

In this paper a physical model for simulating district heating networks was proposed and successfully applied to the test case of the Tannheim district heating system. The model is available to predict temperature and flows at the consumer installations with minimal average error. It has, however, problems with certain transient behavior. This leaves room for further improvements, which will be addressed in future work.

References

[1] P. Pinson, T.S. Nielsen, H.Aa. Nielsen, N.K. Poulsen and H. Madsen, Temperature prediction at critical points in district heating systems, *European Journal of Operational Research*, vol. 194, pp. 163-176, 2009

[2] E. Dotzauer, Simple model for prediction of loads in district heating systems, *Applied Energy* 73, 277-284, 2002

[3] K. Kato, M. Sakawa, K. Ishimaru, S. Ushiro and T. Shibano, Heat Load Prediction through Recurrent Neural Networks in District Heating and Cooling Systems, *IEEE International Conference on Systems, Man and Cybernetics*, pp. 1401-1406, 2008

[4] L. Haiyan, P. Valdimarsson, District Heating Modeling and Simulation, *Thirty-Fourth Workshop on Geothermal Reservoir Engineering Stanford University*, Stanford, California, February 9-11, 2009

[5] H.V. Larsen, H. Pàlsson, B. Bøhm, H.F. Ravn, Aggregated dynamic simulation model of district heating networks, *Energy Conversion and Management*, vol. 43, pp 995-1019, 2002

[6] G. Sandou, S. Font, S. Tebbani, A. Hiret and C. Mondon, Predictive Control of a Complex District Heating Network, *Proceedings of the 44th IEEE Conference on Decision and Control*, Spain, pp. 12-15, December, 2005

[7] H. Pàlsson, Methods for planning and operating decentralized combined heat and power plants. Department of Energy Engineering, Technical University of Denmark and Systems Analysis Department, Riso National Laboratory, *Report 1185*, 2000.

[8] F. M. White, *Fluid Mechanics* 4th ed., McGraw-Hill Series in Mechanical Engineering, 1998.

[9] C. E. Frouzakis, Y. G. Kevrekidis, J. Lee, K. Boulouchos and A. A. Alonso, Proper Orthogonal Decomposition of Direct Numerical Simulation Data, *Proceedings of the Combustion Institute*, vol. 28, pp. 75-81, 2000

[10] R. Courant, K. Friedrichs and H. Lewy, On the partial difference equations of mathematical physics, *IBM J. Res. Develop.*, 11, pp. 215-234, 1967

[11] I. Gabrielaitiene, B. Bøhm and B. Sunden, Modelling temperature dynamics of a district heating system in Naestved, Denmark - A case study, *Energy Conversion and Management*, vol. 48, pp. 78-86, 2008

[12] E. Hairer, G. Wanner, *Solving Ordinary Differential Equations II*, Springer, 1991

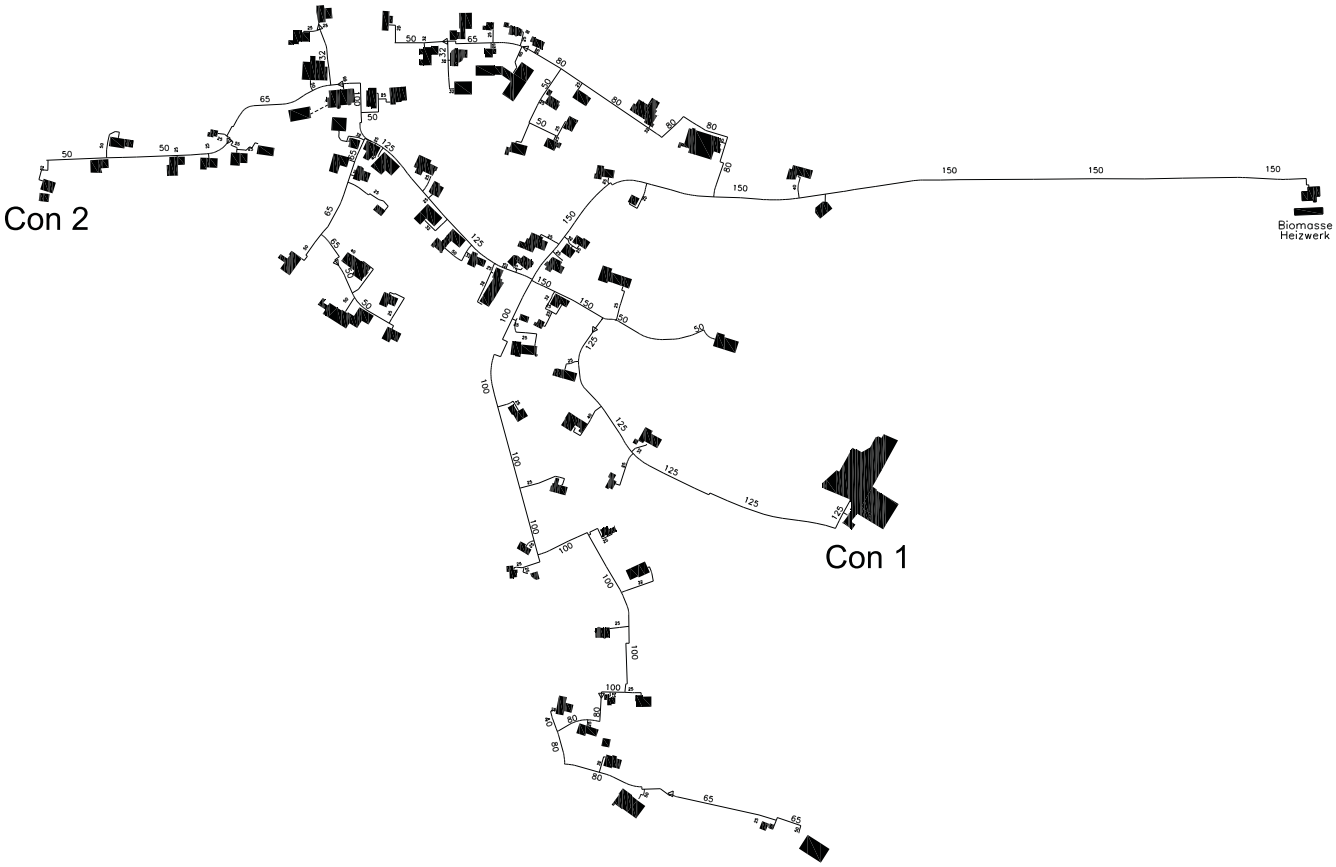

Figure 11: District heating network Tannheim.